Clinical Cancer Research

PRMT5 Circular RNA Promotes Metastasis of Urothelial Carcinoma of the Bladder through Sponging miR-30c to Induce Epithelial–Mesenchymal Transition

Xin Chen[1,2], Ri-Xin Chen[1], Wen-Su Wei[1,2], Yong-Hong Li[1,2], Zi-Hao Feng[3], Lei Tan[1,2], Jie-Wei Chen[1,4], Gang-Jun Yuan[1,2], Si-Liang Chen[1,2], Sheng-Jie Guo[1,2], Kang-Hua Xiao[1,2], Zhuo-Wei Liu[1,2], Jun-Hang Luo[3], Fang-Jian Zhou[1,2], and Dan Xie[1,4]

Abstract

Purpose: Circular RNAs (circRNAs), a novel class of noncoding RNAs, have recently drawn lots of attention in the pathogenesis of human cancers. However, the role of circRNAs in cancer cells epithelial–mesenchymal transition (EMT) remains unclear. In this study, we aimed to identify novel circRNAs that regulate urothelial carcinoma of the bladder (UCB) cells' EMT and explored their regulatory mechanisms and clinical significance in UCBs.

Experimental Design: We first screened circRNA expression profiles using a circRNA microarray in paired UCB and normal tissues, and then studied the clinical significance of an upregulated circRNA, circPRMT5, in a large cohort of patients with UCB. We further investigated the functions and underlying mechanisms of circPRMT5 in UCB cells' EMT. Moreover, we evaluated the regulation effect of circPRMT5 on miR-30c, and its target genes, *SNAIL1* and *E-cadherin*, in two independent cohorts from our institute and The Cancer Genome Atlas (TCGA).

Results: We demonstrated that upregulated expression of circPRMT5 was positively associated with advanced clinical stage and worse survival in patients with UCB. We further revealed that circPRMT5 promoted UCB cell's EMT via sponging miR-30c. Clinical analysis from two independent UCB cohorts showed that the circPRMT5/miR-30c/SNAIL1/E-cadherin pathway was essential in supporting UCB progression. Importantly, we identified that circPRMT5 was upregulated in serum and urine exosomes from patients with UCB, and significantly correlated with tumor metastasis.

Conclusions: CircPRMT5 exerts critical roles in promoting UCB cells' EMT and/or aggressiveness and is a prognostic biomarker of the disease, suggesting that circPRMT5 may serve as an exploitable therapeutic target for patients with UCB. *Clin Cancer Res; 24(24); 6319–30. ©2018 AACR.*

Introduction

Urothelial carcinoma of the bladder (UCB) is one of the most common malignancies worldwide with a high rate of recurrence (1). Around 70% of the patients are diagnosed with a non–muscle-invasive tumor (NMIBC) and 30% with a muscle-invasive tumor (MIBC). Fifty percent of the patients with MIBC develop distant metastases in the lungs, bones, and liver and result in poor prognosis (2). Until now, no effective therapies are available for patients with UCB with tumor metastasis. Therefore, a better understanding of the molecular mechanisms that drive tumorigenesis and/or progression in UCB is critical to develop more efficient anticancer treatments.

Circular RNAs (circRNAs) are a class of small RNAs with covalently closed loop structure that are formed from exon "skipping" and "direct back-splicing" of pre-mRNA transcripts (3, 4). During the past 20 years, circRNAs have occasionally been identified from a few transcribed genes (5, 6), as nonfunctional "junk" RNA molecules. Recently, with the development of deep RNA sequencing, a large number of exonic and intronic circRNAs have been identified across the eukaryotic linage (7–9), indicating that circRNAs are not simply byproducts of splicing errors, rather, they have multiple regulatory roles.

CircRNA expression is dynamic, displaying varying levels and ratios under different pathologic environments. Emerging evidence suggests that some circRNAs function as miRNA sponges to trap miRNA involved in tumorigenesis. It has been reported that ciRS-7 serves as miR-7 sponge to regulate the expression of several oncogenes (10), and circHIPK3 is a sponge of miR-124 to suppress cell proliferation in multiple cancers (11). CircRNA sequencing revealed a circRNA SMARCA5/miR-17-3p/miR-181b-5p axis

[1]State Key Laboratory of Oncology in South China; Collaborative Innovation Center for Cancer Medicine; Sun Yat-Sen University Cancer Center, Guangzhou, China. [2]Department of Urology, Sun Yat-Sen University Cancer Center, Guangzhou, China. [3]Department of Urology, the First Affiliated Hospital, Sun Yat-Sen University, Guangzhou, China. [4]Key Laboratory of Protein Modification and Degradation, School of Basic Medical Sciences, Affiliated Cancer Hospital & Institute of Guangzhou Medical University, Guangzhou, China.

Note: Supplementary data for this article are available at Clinical Cancer Research Online (http://clincancerres.aacrjournals.org/).

X. Chen, R.-X. Chen, W.-S. Wei, Y.-H. Li, and Z.-H. Feng contributed equally to this article.

Corrected online March 23, 2021.

Corresponding Authors: Dan Xie, Sun Yat-Sen University Cancer Center, No. 651 DongFeng Road East, Guangzhou, Guangdong 510060, China. Phone: 8620-8734-3193; Fax: 8620-7734-3170; E-mail: xiedan@sysucc.org.cn; and Fang-Jian Zhou, zhoufj@sysucc.org.cn

doi: 10.1158/1078-0432.CCR-18-1270

Translational Relevance

Recently, dysregulated circular RNAs (circRNAs) and their roles in cancer have attracted much attention. However, the functional and clinical significance of circular RNAs in cancer cells' epithelial–mesenchymal transition (EMT) progression remains unclear. Herein, we found circPRMT5 was frequently overexpressed in urothelial carcinoma of the bladder (UCB) tissues, and its upregulated expression was associated with advanced clinical stage and/or worse patient survival. Functional and mechanistic assays in UCB cell lines and a xenograft mouse model revealed that circPRMT5 promoted cancer cells' EMT process and led to an aggressive phenotype through blocking tumor-suppressive effects of miR-30c. Importantly, we demonstrated that circPRMT5 was upregulated in serum and urine exosomes from patients with UCB, and correlated with cancer metastasis. Collectively, we identified that circPRMT5 is a promising prognostic biomarker for patients with UCB and provided first line of evidence that this circular RNA may be a potential target for new treatment modalities in UCBs.

in the pathogenesis of hepatocellular carcinoma, providing novel promising markers for cancer diagnosis and therapy (12). To date, however, the functions and underlying mechanisms of certain dysregulated circRNAs in the epithelial–mesenchymal transition (EMT) process of human cancers, such as UCB, remain largely unknown.

Exosomes are membrane vesicles of an average 30- to 100-nm diameter (13), containing miRNA, mRNA, and proteins, and are released by cells into the extracellular microenvironment (14). Recently, it has been shown that circRNAs can be secreted by serum exosome from cancer cells into circulation, with unknown pathologic functions (15, 16). Because patients with UCB have increased numbers of exosomes in the blood and urine (17, 18), it is interesting to investigate the function of circRNAs and their clinical significance in the exosomes derived from UCB tissues.

In this study, we identified that circPRTM5 was one of the critical circRNAs that was frequently upregulated in UCB tissues by using a circRNA microarray profiling. Patients with UCB with higher expression of circPRMT5 were positively associated with poorer survival. Further mechanism-of-action studies demonstrated that circPRMT5 promoted UCB cells' EMT both *in vivo* and *in vitro* via sponging miR-30c. Furthermore, we revealed, for the first time, that circPRMT5 was upregulated in serum and urine exosomes from patients with UCB, and predicted UCBs metastasis. In conclusion, our study demonstrates that circPRMT5 exerts critical regulatory role in the EMT process and consequent aggressiveness of UCB cells.

Materials and Methods

UCB patient samples

For circRNA expression profiling and IHC analysis, a cohort of UCB tissues with matched adjacent normal bladder tissues was derived from 119 patients with UCB who had received radial cystectomy at Sun Yat-Sen University Cancer Center (SYSUCC, Guangzhou, Guangdong, China), from 2005 to 2012. Clinical information of the patients with UCB was summarized in Supplementary Table S1. All patients were followed up on regular basis and disease-free survival (DFS) time was determined from the date of surgery to the date of the first clinical evidence of cancer recurrence, and was censored at the date of death from other causes or the date of the last follow-up visit for survivors. For exosome purification, serum and urine samples were collected from patients with UCB and healthy donors from 2015 to 2017. All specimens were snap frozen in liquid nitrogen upon collection for further use. Tumor stage was defined according to the criteria of the sixth edition of the TNM classification of the International Union Against Cancer (UICC, 2009; ref. 19). This study has been approved by Institutional Review Board of SYSUCC, and the study was informed in accordance with Declaration of Helsinki. Written informed consent was obtained from the patients before the study began.

The care and maintenance of animals

All procedures involving mouse were approved by the Institutional Animal Care and Use Committee of SYSUCC. All mice were obtained from Charles River Laboratories. *In vivo* metastasis model was established by intravenous injection of 5×10^5 UCB cells through the tail vein into each 4-week-old BALB/c nude mice. Six weeks after injection, the mice were sacrificed. The lungs were removed and fixed with phosphate-buffered formalin. Subsequently, consecutive tissue sections were made for each block of the lung. The numbers of pulmonary metastatic nodules in the lung were carefully examined.

Cell lines and cell culture

Four UCB cell lines (i.e., T24, TCC-SUP, 5637, and UM-UC-3) and a nontumorous bladder cell line, SV-HUC-1, were purchased from ATCC in 2013. The BIU cell line was obtained from the Institute of Urology at the first affiliated hospital of Peking University (Beijing, China) as a gift in 2012. UM-UC-3 line was cultured in DMEM (Invitrogen) supplemented with 10% FBS (HyClone). The other five lines were cultured in RPMI1640 (Invitrogen) supplemented with 10% FBS (HyClone). All cell lines used in this study were authenticated 3 months before the beginning of the study (2014) based on viability, recovery, growth, and morphology by the manufacturer and all the cell lines were not cultured for than 2 months (20).

Data availability

Microarray data are accessible using GEO ID: GSE112719.

Statistical analysis

Statistical analysis in SYSUCC cohorts was carried out with SPSS software (SPSS Standard version 13.0; SPSS Inc.). The χ^2 test was used to assess the statistical significance of the association of the expression of circPRMT5 with the patient's clinicopathologic parameters and its correlation. Comparisons between groups for statistical significance were performed with the independent-sample *t* test. DFS was assessed with the Kaplan–Meier method and compared by the log-rank test. Correlations were analyzed by Pearson correlation test. *P* values of <0.05 were considered significant. All statistical analyses were carried out using GraphPad Prism version 6.0. The data were shown as mean ± SD in the bar charts and the difference was calculated by either Student *t* test or χ^2 test. Pearson coefficient was applied to analyze the correlations. Survival analysis was performed by Kaplan–Meier curves and log-rank test for significance. *P* values of <0.05 were considered statistically significant.

To detect outliers in related molecular correlation analysis in UCB cohort from the Cancer Genome Atlas (TCGA), we performed the Tukey box-plot method of inner and outer "fences" to identify the outliers. If the expression level of SNAIL1, miR-30c, or E-cadherin for a UCB sample was either under the 1.5 interquartile range (IQR) of the lower quartile, or above the 1.5 IQR of the upper quartile, these samples were regarded as the outliers and were excluded from further analysis. R software version 3.3.1 (R Foundation for Statistical Computing) was used for performing statistical tests and plotting.

Results

Expression profiles of circRNAs in human UCB tissues

To investigate circRNA expression profile in UCB tissues, we compared three pairs of UCB tissue and their matched nontumor tissue samples by using circRNA microarray. Between UCB tissues and noncancerous matched tissues, the variation of circRNA expression was demonstrated in the volcano plot. As a result, 37 circular RNAs were upregulated, whereas 43 circular RNAs were downregulated on the basis the $\log_2$ (fold changes) ≥ 1, $P < 0.05$, and FDR < 0.05 (Fig. 1A). In summary, 33 exonic, one intronic, and three intragenic circRNAs were noted among upregulated circRNAs, whereas 35 exonic, five intronic, one intragenic, and two antisense circRNAs were noted among downregulated circRNAs (Supplementary Table S2). The top 15 upregulated and downregulated circRNAs were shown by hierarchical clustering (Fig. 1B).

Characterization of circPRMT5 in UCBs

In this study, circRNA_101320 (chr14:23395341-23396023) was evaluated as the most highly upregulated circRNA in UCBs, with more than sixfold change from microarray analysis. By browsing the human reference genome (GRCh37/hg19), we identified that circRNA_101320 is derived from PRMT5, which is located on chromosome 14q11.2, and thus we named it circPRMT5. To investigate the clinical significance of circPRMT5 expression in patients with UCB, we further collected 119 pairs of UCB and matched normal bladder tissue samples, respectively. By using qRT-PCR, we validated that the expression of circPRMT5 was frequently overexpressed in UCBs compared with that in matched nontumor tissues (Fig. 1C, left). In addition, the upregulated expression of circPRMT5 was more likely to occur in patients with lymph node metastasis compared with that without metastasis (Fig. 1C, right). Further statistical analyses evaluated that high expression of circPRMT5 in UCBs was positively associated with an advanced T and N status (Supplementary Table S1), and displayed poorer DFS (Fig. 1D).

We next aimed to characterize this circRNA in UCB cells. Compared with SV-HUC-1 cell line (an uroepithelium cell line), the expression of circPRMT5 was clearly upregulated in five UCB cell lines examined (Supplementary Fig. S1A). Because T24 cells expressed the highest amount of circPRMT5, it was chosen for the next study. We further analyzed circPRMT5 by RT-PCR, Sanger sequencing (Fig. 1E), and northern blot analysis (Fig. 1F) in T24 cells, according to previously described methodology (21). After examination by RT-PCR with divergent primers, the sequenced PCR product was corresponding from the 5′exon 7, exon 6 to 3′exon 5. We then used the probe hybridizing with exon 7–exon 5 junction to identify circPRMT5, and meanwhile, we used the probe hybridizing with exon 7 to identify both circPRMT5 and PRMT5 (Fig. 1F). Resistance to digestion with RNase R exonuclease confirmed that this RNA species is circular in form (Supplementary Fig. S1B). Notably, the circular isoform is highly stable, with transcript half-life exceeding 24 hours (Supplementary Fig. S1C) in T24 cells. These data demonstrated that circPRMT5 contained three circularized exons, formed from exon back-splicing. Further examination by mRNA fractionation (Fig. 1G) and FISH (Fig. 1H) revealed that the majority of circPRMT5 preferentially localized in the cytoplasm. Taken together, our results show that circPRMT5 is an abundant and stable circRNA expressed in UCB cells.

To determine whether nor not the circPRMT5 was present in other types of human carcinomas, we further examined the expression of circPRMT5 in a series of lung, liver, and colorectal carcinoma tissues. The expression levels of circPRMT5 were not significantly increased in these cancer tissues (Supplementary Fig. S1D). These results, together, suggested the upregulated circPRMT5 expression in UCBs may be a tumor-specific event.

CircPRMT5 promotes UCB cells' aggressiveness

We determined to evaluate the biological roles of circPRMT5 in UCB. We first constructed shRNA, which covered the back-splicing region of circPRMT5 for silencing. The results showed that depletion of circPRMT5 with short hairpin RNAs resulted in a clear decrease in its mRNA levels. We further examined the 5′ neighboring genes of PRMT5 and found that knockdown of circPRMT5 or overexpression of circPRMT5 had no effect on the neighboring genes (Fig. 2A and B). However, silence of circPRMT5 could significantly inhibit UCB cells' migration and invasive capacities (Fig. 2C and E; Supplementary Fig. S2A). On the other side, ectopic overexpression of circPRMT5 in UCB 5637 cells substantially increased cell migration and invasion abilities (Fig. 2D and F; Supplementary Fig. S2B).

Subsequently, to evaluate the role of circPRMT5 in tumor metastasis *in vivo*, BALB/c nude mice were injected intravenously in the tail vein with T24 cells, stably expressing either control or circPRMT5 shRNA. Six weeks after cell injection, mice were killed and metastatic tumor nodules formed in the lung were examined. We showed that the mice injected with cells with circPRMT5 shRNA had less metastatic nodules in the lung than mice injected with control cells (Fig. 2G). Whereas, mice injected with cells with stable overexpression of circPRMT5 markedly increased tumor nodules in the lung as compared with that of controls (Fig. 2H).

CircPRMT5 induces UCB cells' EMT

It is known that EMT is a critical process that induces aggressiveness in cancer cells. Therefore, we assessed whether circPRMT5 could enhance UCB cells' EMT phenotype. Western blot analysis (WB) showed that in the knockdown of circPRMT5 in UCB cells, the expression of the epithelial marker, E-cadherin was increased, whereas the expression of the mesenchymal markers, Vimentin and N-cadherin, were all decreased (Fig. 3A). On the contrary, overexpression of circPRMT5 led to the downregulated expression of E-cadherin, and upregulated expression of vimentin and N-cadherin in UCB cells (Fig. 3B).

Furthermore, immunofluorescence (IF) staining confirmed the upregulated expression of E-cadherin and downregulated expression of vimentin and N-cadherin in circPRMT5-silenced UCB cells (Fig. 3C), whereas overexpression of circPRMT5 was accompanied with the increased expression of vimentin and N-cadherin in the cells (Fig. 3D). These findings indicated that

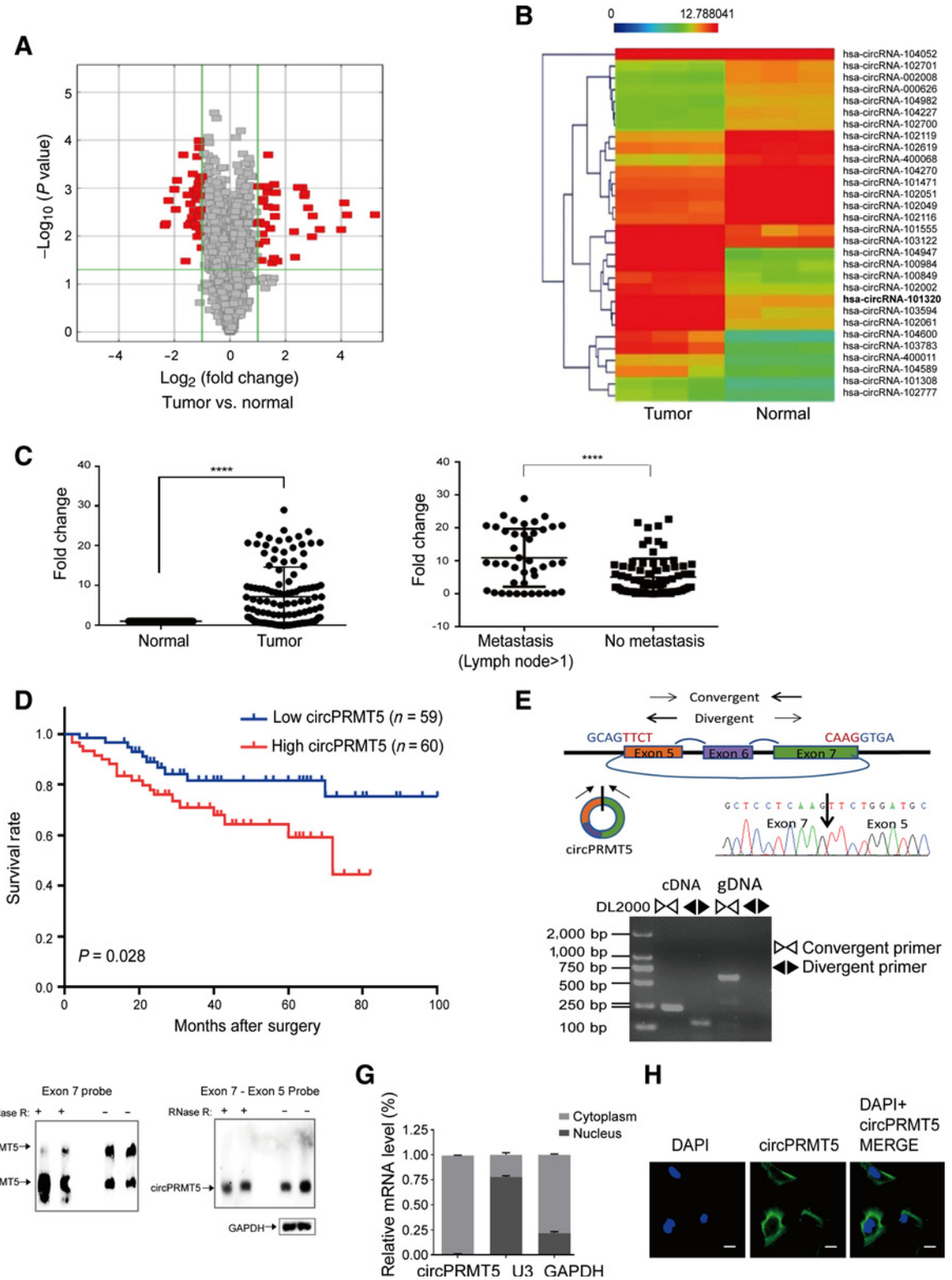

Figure 1.

CircPRMT5 was overexpressed in UCBs and correlates with poor patient prognosis. **A,** Volcano plot compared the expression fold changes of circRNAs for UCB tissues versus adjacent normal bladder tissues. The red dots represent significantly expression changed circRNAs. **B,** Clustered heatmap for tissue-specific circRNAs from three human normal tissues, with rows representing circRNAs and columns representing tissues. The circRNAs were classified according to the Pearson correlation. The numerical data represented the serial number of circRNAs in circBase. (*Continued on the following page.*)

circPRMT5 promoted UCB cells' EMT. Furthermore, our results showed that the expression level of the host gene, *PRMT5*, was not changed by either knockdown or overexpression of circPRMT5 in UCB cells, suggesting that the pathologic role of circPRTM5 in promoting EMT is not dependent on PRMT5.

CircPRMT5 serves as a sponge for multiple miRNAs in UCBs

Given that circRNA has been shown to act as miRNA sponge (10) and circPRMT5 is abundant and stable in the cytoplasm, we wondered whether circPRMT5 can bind to certain miRNAs in the pathogenic process of UCB. We first assessed the occupancy of AGO2 in the region of circPRMT5. By RNA immunoprecipitation for AGO2 in T24 cells stably expressing Flag-AGO2 and Flag-GFP, we observed that endogenous circPRMT5 pulled-down from Flag-AGO2 cells was specifically enriched by qRT-PCR analysis (Fig. 4A), suggesting that circPRMT5 is incorporated into the RNA-induced silencing complex (RISC complex). To identify whether certain miRNAs can bind to circPRMT5, we further constructed a circPRMT5 fragment and inserted it downstream of the luciferase reporter gene. Transfection of circPRMT5 shRNA could efficiently decrease the luciferase activity of circPRMT5 reporter gene (Fig. 4B).

To identify the miRNAs that bind to circPRTM5, we performed a luciferase screening with a miRNA mimic library. Eighty-three miRNA mimics were cotransfected with the circPRMT5 luciferase reporters into T24 cells (Fig. 4C), respectively. Compared with the control miRNA, five miRNAs, that is, miR-30c, miR-335, miR-188, miR-377, and miR-597, were able to reduce at least half of the luciferase reporter activities (Fig. 4C). Using the TargetScan miRNA prediction programs (22), the five miRNAs were found to contain at least one to two binding sites for the circPRMT5 region (Fig. 4D; Supplementary Fig. S3). By mutating each miRNA target site from the luciferase reporter with circPRTM5 sequence in the 3′ untranslated region (UTR), we further observed that transfection of the miRNA had no significant effect on luciferase activity, when the miRNA target sites were mutated from the luciferase reporter (Fig. 4E). These results suggest that circPRMT5 may function as a sponge to these five miRNAs.

To fish out the bona fide miRNAs that interact with circPRMT5 in UCB cells, we used a biotin-labeled circPRMT5 probe to perform RNA *in vivo* precipitation (RIP). Only a twofold enrichment of miR-30c, but not the other four miRNAs, was copurified with biotin-labeled circPRMT5 probe, compared with the negative control (Fig. 4F). Once circPRMT5 was silenced, the enrichment of miR-30c in circPRMT5 probe pull-down fraction was largely diminished (Fig. 4G). Meanwhile, we found that the endogenous and exogenous expressed circPRMT5 were colocalized with miR-30c by using RNA–FISH assay (Fig. 4H). These results taken together, provided evidences that circPRMT5 could directly bind miR-30c. Therefore, we selected miR-30c as the target of circPRMT5 for further investigation.

CircPRMT5 promotes UCB cells aggressiveness and EMT by reducing the inhibitory effect of miR-30c by sponge activity

To investigate whether or not circPRMT5 exerted its oncogenic effect through sponge activity of miR-30c, the inhibitor of miR-30c was used to examine whether the effect of circPRMT5 depletion can be rescued by miR-30c inhibitor. The results showed that miR-30c inhibitor could functionally restore circPRMT5 silence-suppressed UCB cells' migration and invasive abilities (Fig. 5A and C; Supplementary Fig. S4A and S4C). On the other hand, miR-30c mimics can substantially prevent circPRMT5 overexpression–enhanced UCB cells migration and invasion (Fig. 5B and D; Supplementary Fig. S4B and S4D).

Our *in vivo* mouse model studies also supported the view that the oncogenic role of circPRMT5 in UCB metastasis was dependent on the sponge activity of miR-30c. The decreased metastatic nodules in the lung formed by injection with the circPRMT5-silenced UCB cells, were largely restored by treatment of miR-30c inhibitor (Fig. 5E); whereas the increased metastatic nodules in the lung formed by circPRMT5-overexpressed cells of were remarkable abrogated by miR-30c mimic (Fig. 5F).

On the basis of our data that circPRMT5 can effectively quench the function of miR-30c to promote UCB cells' EMT progression, we therefore hypothesized that circPRMT5 may be responsible for enhancing the expression levels of miR-30c downstream targets by acting as a miR-30c sponge. Using miRanda analysis (23), we showed that miR-30c can directly target the 3′UTR of *SNAIL1* (Supplementary Fig. S5A), a critical transcription factor that promotes cell's EMT. Moreover, transfection of miR-30c mimics substantially could downregulate the expression of SNAIL1 in UCB cells, suggesting that SNAIL1 is a bona fide target of miR-30c (Supplementary Fig. S5B).

Our further studies showed that silence of circPRMT5 could lead to an apparent downregulation of SNAIL1, and meanwhile, the levels of E-cadherin, a well-known downstream target of SNAIL1 (24), were substantially increased. In addition, the reduction of SNAIL1, as well as the increased E-cadherin levels, accompanied with the altered mesenchymal markers, vimentin and N-cadherin, was largely prevented after the treatment of miR-30c inhibitor in circPRMT5-silenced UCB cells (Fig. 5G and H), whereas, treatment of miR-30c mimics in circPRMT5-overexpressed cells may lead to the opposite effect on the expression of SNAIL1, E-cadherin, vimentin, and N-cadherin (Fig. 5I and J). These results, collectively, revealed that circPRMT5 promoted UCB cells' EMT and aggressiveness through reducing the inhibitory effect of miR-30c by sponge activity.

CircPRMT5 regulates the miR-30c/SNAIL1/E-cadherin pathway and promotes EMT in UCB cells

Given the important role of circPRMT5 via sponging miR-30c in UCB cells' EMT and aggressive potential, we then analyzed the clinical significance of the circPRMT5/miR-30c/SNAIL1/E-cadherin

(*Continued*.) **C,** Scatter plots illustrating qRT-PCR analysis of expression fold change for circPRMT5 in UCB tissues compared with matched adjacent normal bladder tissues from the SYSUCC (left); and the expression fold change for circPRMT5 in UCB tissues with lymph node metastasis compared with those without metastasis from the SYSUCC (right). ****, $P < 0.0001$, paired Student *t* test. **D,** Kaplan–Meier curves with univariate analyses of DFS (*, $P < 0.05$, log-rank analysis) in patients with UCB with low versus high expression of the circPRMT5 from SYSUCC cohorts. **E,** Verification that circPRMT5 is a circRNA, using divergent and convergent primers. Top, schematic illustration of circPRMT5 locus with specific primers. Bottom, RT-PCR products with divergent primers showing circularization of circPRMT5. gDNA, genomic DNA. Middle, Sanger sequencing result of circPRMT5. **F,** Northern blot analysis of circPRMT5 and PRMT5 transcripts with the probes hybridizing with exon 7 (left) and exon 7–exon 5 junction (top right) in the presence or absence of RNase R treatment, respectively. GAPDH mRNA was also blotted as the control (bottom right). **G,** Cytoplasmic and nuclear mRNA fractionation experiment showed that circPRMT5 is mainly located in the cytoplasm. The amount of circPRMT5 was normalized to the value measured in the cytoplasm. Data are the mean ± SD of three experiments. **H,** Representative FISH images of circPRMT5, showing localization of circPRMT5 in the cytoplasm of T24 cells. Scale bars, 10 μm. For **F** and **H**, junction probe is complementary to the junction sequences of circPRMT5.

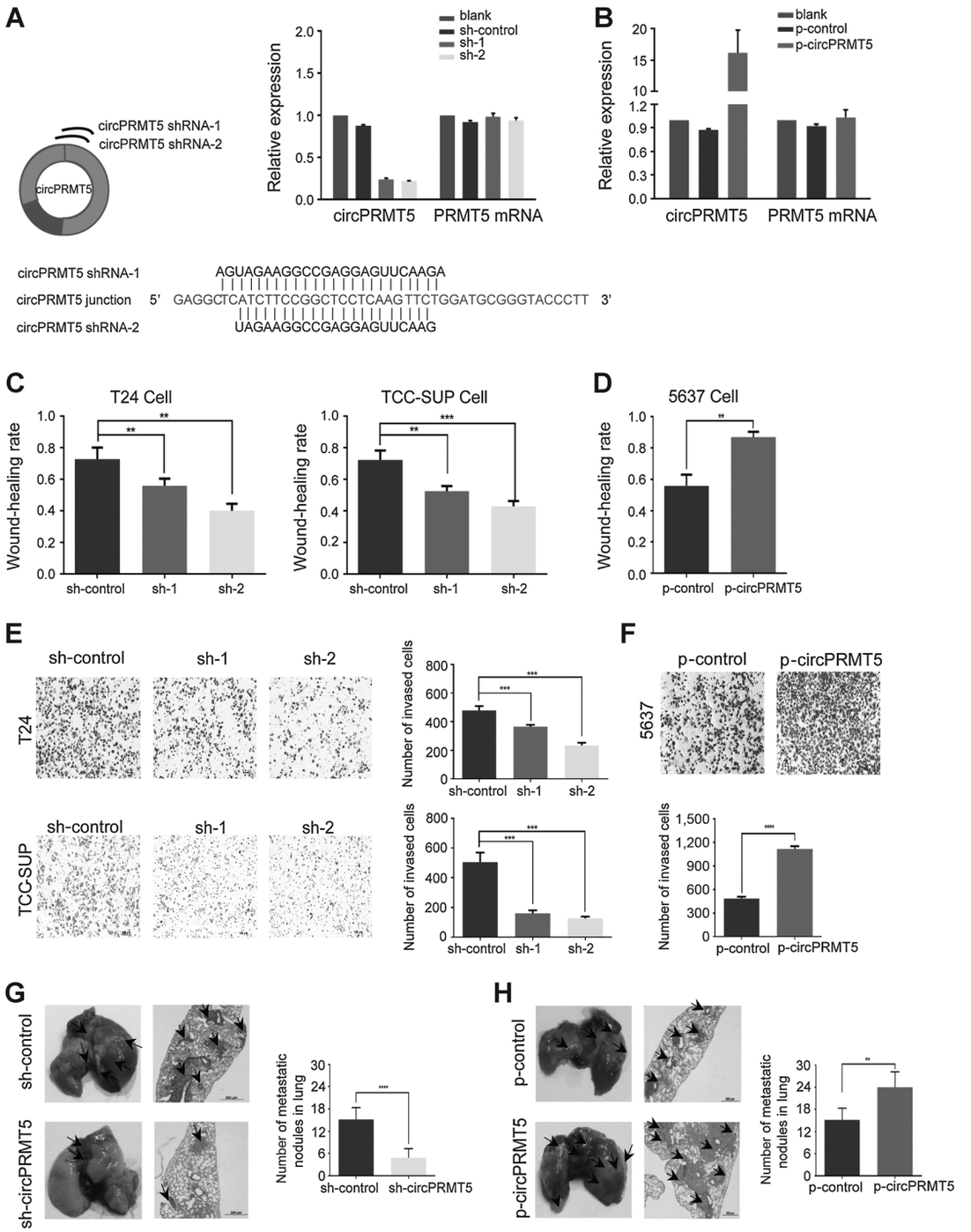

Figure 2.

Silencing of circPRMT5 RNA inhibited UCB cells' invasion. **A,** Schematic illustration showed two targeted shRNAs. Sh-circPRMT5 targets the back-splice junction of circPRMT5 (left). qRT-PCR for circPRMT5 and PRMT5 mRNA in UCB cells treated with two shRNAs as described above. Data are the mean ± SD of three experiments. **B,** qRT-PCR for circPRMT5 and PRMT5 mRNA in UCB cells transfected with control vector or circPRMT5 overexpression plasmid. Data are the mean ± SD of three experiments. **C,** Wound-healing assay showed that knockdown of circPRMT5 inhibited the migration ability of the indicated UCB cells. **D,** Wound-healing assay analyses showed that overexpression of circPRMT5 promoted the migration ability of the indicated UCB cells. **E,** Transwell assay showed that knockdown of circPRMT5 inhibited the invasion ability of the indicated UCB cells. **F,** Transwell assay showed that overexpression of circPRMT5 promoted the invasion ability of the indicated UCB cells. **G** and **H,** Stably transfected T24 cells with circPRMT5-shRNA (**G**) or overexpression of circPRMT5 (**H**) with their respective control lentivirus were injected into the vein of BALB/c nude mice for 6 weeks. Representative images of lungs (left), metastatic nodules (indicated by arrows), and hematoxylin and eosin (H&E) staining of lung metastatic lesions (middle, original magnification, 100×; scale bar, 100 μm) are shown. The number of metastatic nodules formed in the lungs of BALB/c nude mice is summarized for each group tested ($n = 5$; bottom right; **, $P < 0.01$; ***, $P < 0.001$; ****, $P < 0.0001$).

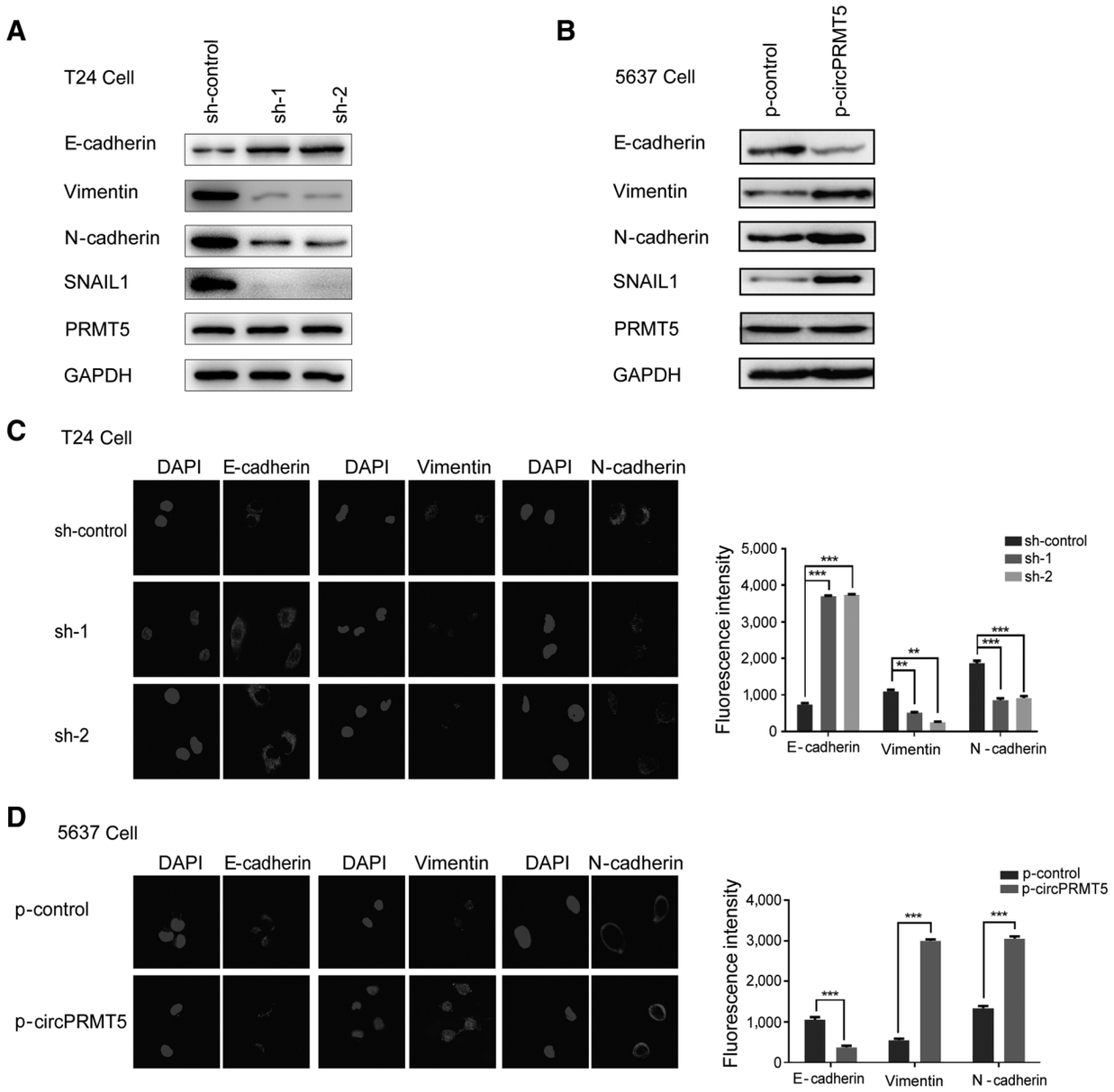

Figure 3.

CircPRMT5 activated the SNAIL1 pathway to induce EMT in UCB cells. **A** and **B,** Western blot analysis comparing circPRMT5-silenced (**A**) and circPRMT5-overexpressing UCB cells (**B**) with their respective control cells were shown for relative expression of E-cadherin, vimentin, N-cadherin, SNAIL1, and PRMT5. GAPDH expression was used as a loading control. **C** and **D,** Representative immunofluorescence (IF) images comparing circPRMT5-silenced (**C**) and circPRMT5-expressing UCB cells (**D**) with their respective control cells were shown for the expression of E-cadherin, vimentin, and N-cadherin. Nuclei were counterstained with DAPI (left). Fluorescence intensity were analyzed by ImageJ. Data are the mean ± SD of three experiments (right; ***, $P < 0.001$).

pathway in patients with UCB. We found that the levels of circPRMT5 were negatively correlated with miR-30c expression in UCBs of SYSUCC cohort (Fig. 6A). Moreover, high-expressed circPRMT5 was significantly correlated with upregulated SNAIL1 and downregulated E-cadherin proteins in the same cohort from SYSUCC (Fig. 6B and C), implying that circPRMT5 is strongly linked to EMT progression in patients with UCB.

To investigate the pathologic role of miR-30c pathway in patients with UCB, we further analyzed the clinical relevance of miR-30c expression in the cohorts derived from TCGA. We evaluated that lower expression of miR-30c was significantly correlated with poorer survival in patients with UCB, and the level of miR-30c may serve as a biomarker of long-term survival (Fig. 6D). In addition, the expression levels of miR-30c were significantly upregulated in the patients without metastasis (Fig. 6E; Supplementary Table S3), which was consistent with the inhibitory function of miR-30c in UCB cells' EMT. Furthermore, the expression levels of miR-30c were negatively correlated with the expression of SNAIL1 in patients with UCB (Fig.

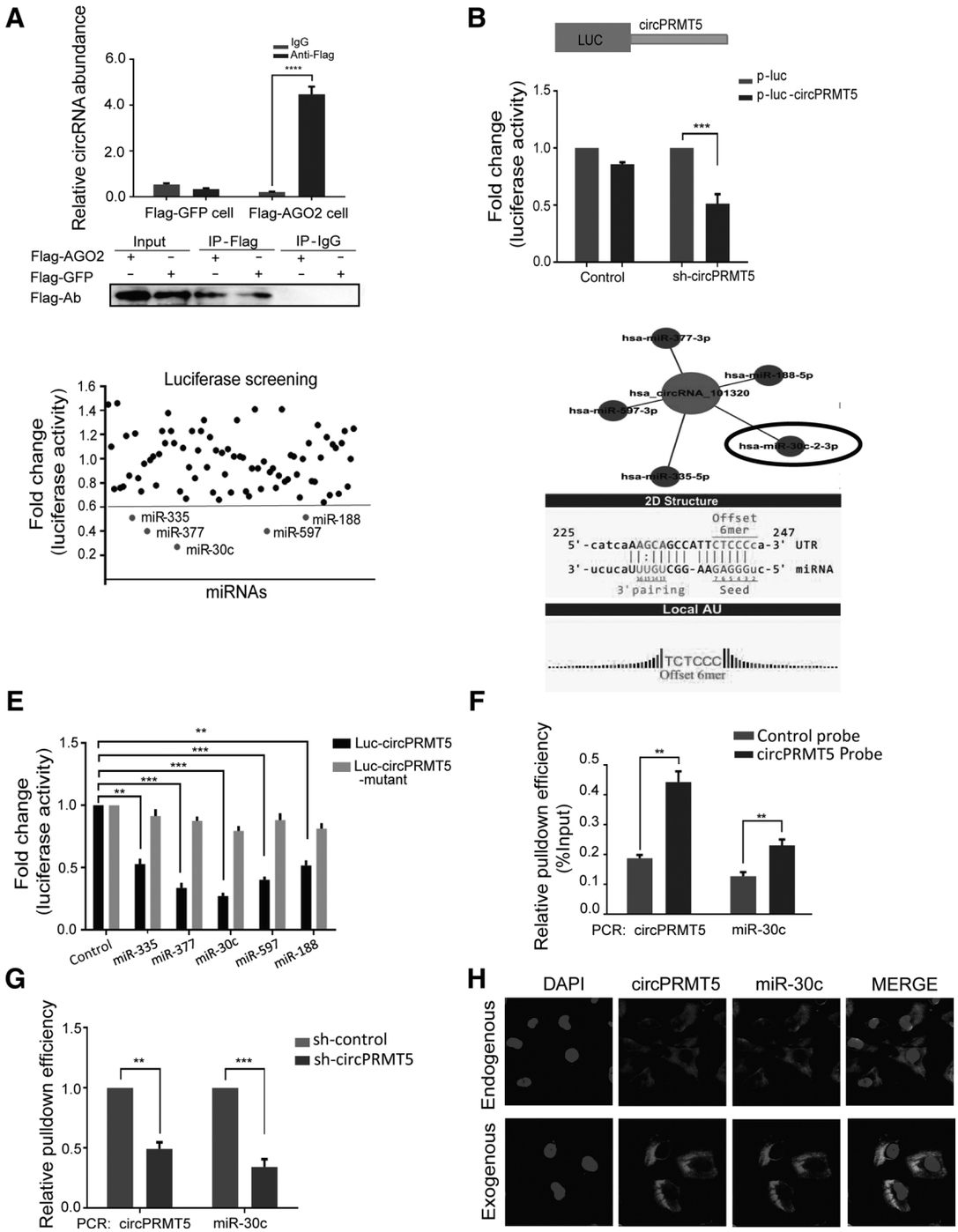

Figure 4.

CircPRMT5 served as a sponge for miR-30c in UCB cells. **A,** Ago2 RIP assay for the amount of circPRM5 in UCB cells expressing Flag-AGO2 or Flag-GFP. Data are the mean ± SD of three experiments. ****, $P < 0.0001$, Student *t* test. **B,** The entire circPRMT5 sequence (red) was cloned into the downstream region of the luciferase gene, denoting LUC-circPRMT5. Luciferase reporter assay for the luciferase activity of LUC-circPRMT5 in T24 cells cotransfected with shRNA against circPRMT5 or control shRNA. Data are the mean ± SD of three experiments. ***, $P < 0.001$, Student *t* test. **C,** Luciferase reporter assay for the luciferase activity of LUC-circPRMT5 in T24 cells transfected with a library of 83 miRNA mimics to identify miRNAs that were able to bind to the circPRMT5 sequence. miRNAs that inhibited luciferase activity by 50% are indicated by red dots. **D,** A schematic drawing showing the putative binding sites of the miRNAs associated with circPRMT5. **E,** Luciferase reporter assay for the luciferase activity of LUC-circPRMT5 or LUC-circPRMT5 mutant in T24 cells cotransfected with miRNA mimics. Data are the mean ± SD of three experiments. **, $P < 0.01$; ***, $P < 0.001$, Student *t* test. **F,** RNA pull-down assay for the amount of circPRMT5 and miR-30c with either circPRMT5 or control probe in UCB cells. RNAs that were pulled down were compared with a 10-fold dilution of input RNA and defined as percentage of input (%input). Data are normalized to that with control probe, showing the mean ± SD of three experiments. **, $P < 0.01$; ***, $P < 0.001$, Student *t* test. **G,** RNA pull-down assay for the amount of circPRMT5 and miR-30c with circPRMT5 probe in UCB cells expressing either control or circPRMT5 shRNA. Data are normalized to that with control shRNA, showing the mean ± SD of three experiments. **, $P < 0.01$; ***, $P < 0.001$, Student *t* test. **H,** IF images represented RNA colocalization of circPRMT5 and miR-30c in control cells or circPRMT5-overexpressing cells.

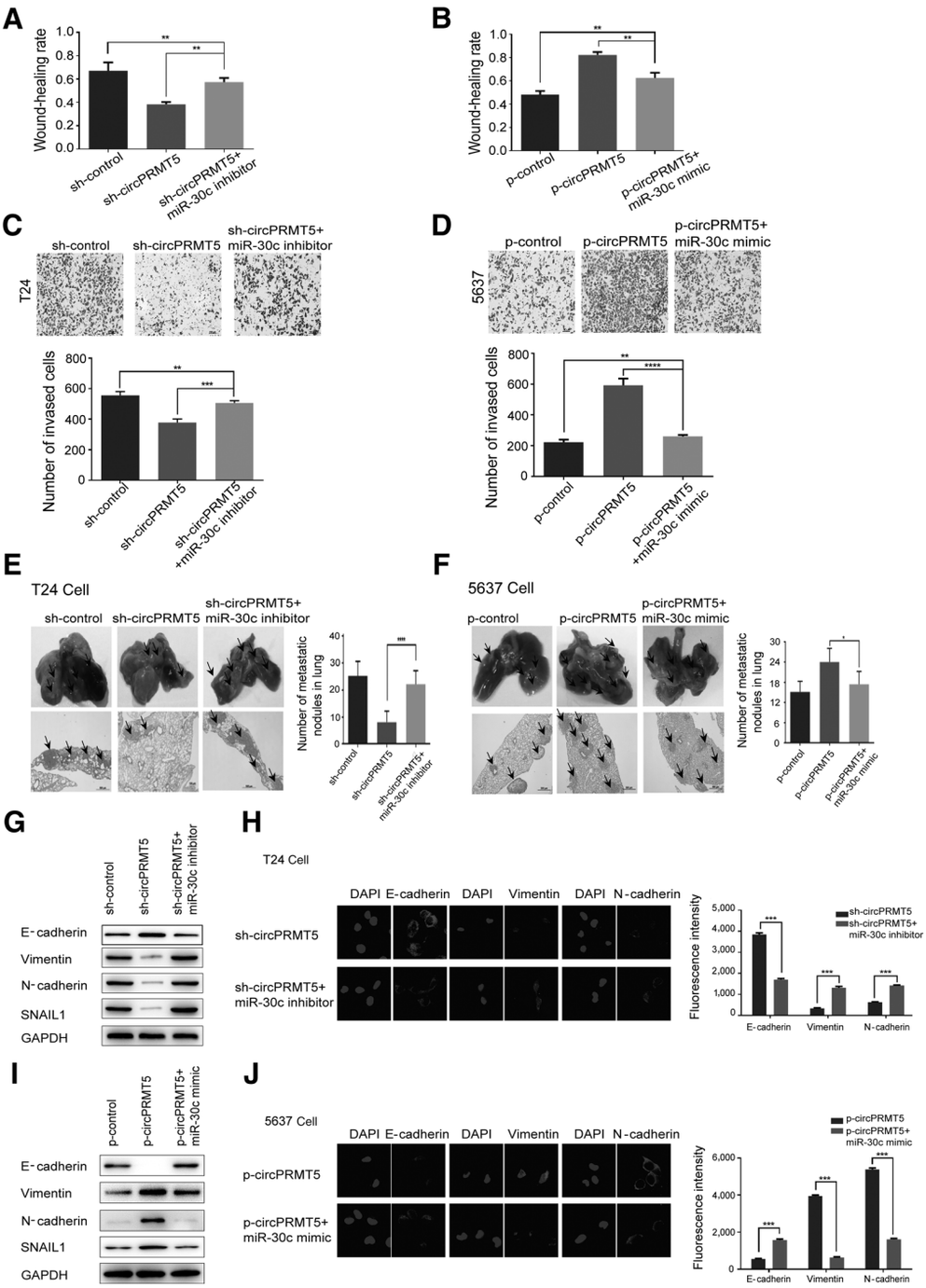

Figure 5.

CircPRMT5 blocked tumor-suppressive effects of miR-30c in UCB cells. **A** and **C,** Knockdown of circPRMT5 inhibited cell migration (**A**) and invasion (**C**) as measured by wound healing and transwell assay in UCB cells. Decreased cell migration and invasion in circPRMT5 knockdown cells was rescued by miR-30c inhibitor. All graphs represent mean ± SE obtained from three independent experiments. **B** and **D,** Overexpression of circPRMT5 promoted cell migration (**B**) and invasion (**D**) as measured by wound healing and transwell assay in UCB cells. Increased cell migration and invasion in circPRMT5 knockdown cells was rescued by miR-30c mimics. **E** and **F,** Representative images of lungs (left), metastatic nodules (indicated by arrows), and H&E staining of lung metastatic lesions (middle, original magnification, 100×; scale bar, 100 μm) are shown. The number of metastatic nodules formed in the lungs of BALB/c nude mice is summarized for each group tested ($n = 5$); bottom right. Compared with the mice injected with circPRMT5-depleted cells that were significantly suppressed, overexpression of miR-30c inhibitor compensated for the inhibitory effect by circPRMT5 depletion in lung metastasis *in vivo* (**E**), whereas overexpression of miR-30c rescued for the enhanced effect by circPRMT5 overexpression on lung metastasis *in vivo* (**F**). **G** and **H,** The expression levels of vimentin, N-cadherin, and SNAIL1/E-cadherin pathway were inhibited by circPRMT5 knockdown, but such repressive effect was abolished by miR-30c inhibitor as observed in Western blot analysis (**G**) and IF (**H**, left). **I** and **J,** The expression levels of vimentin, N-cadherin, and SNAIL1/E-cadherin pathway were enhanced by circPRMT5 overexpression, but such oncogenic effect was inhibited by miR-30c mimics as observed in Western blot analysis (**H**) and IF (**J,** left). Fluorescence intensity presented in **H** and **J** were analyzed by ImageJ. Data are the mean ± SD of three experiments (right; **, $P < 0.01$; ***, $P < 0.001$).

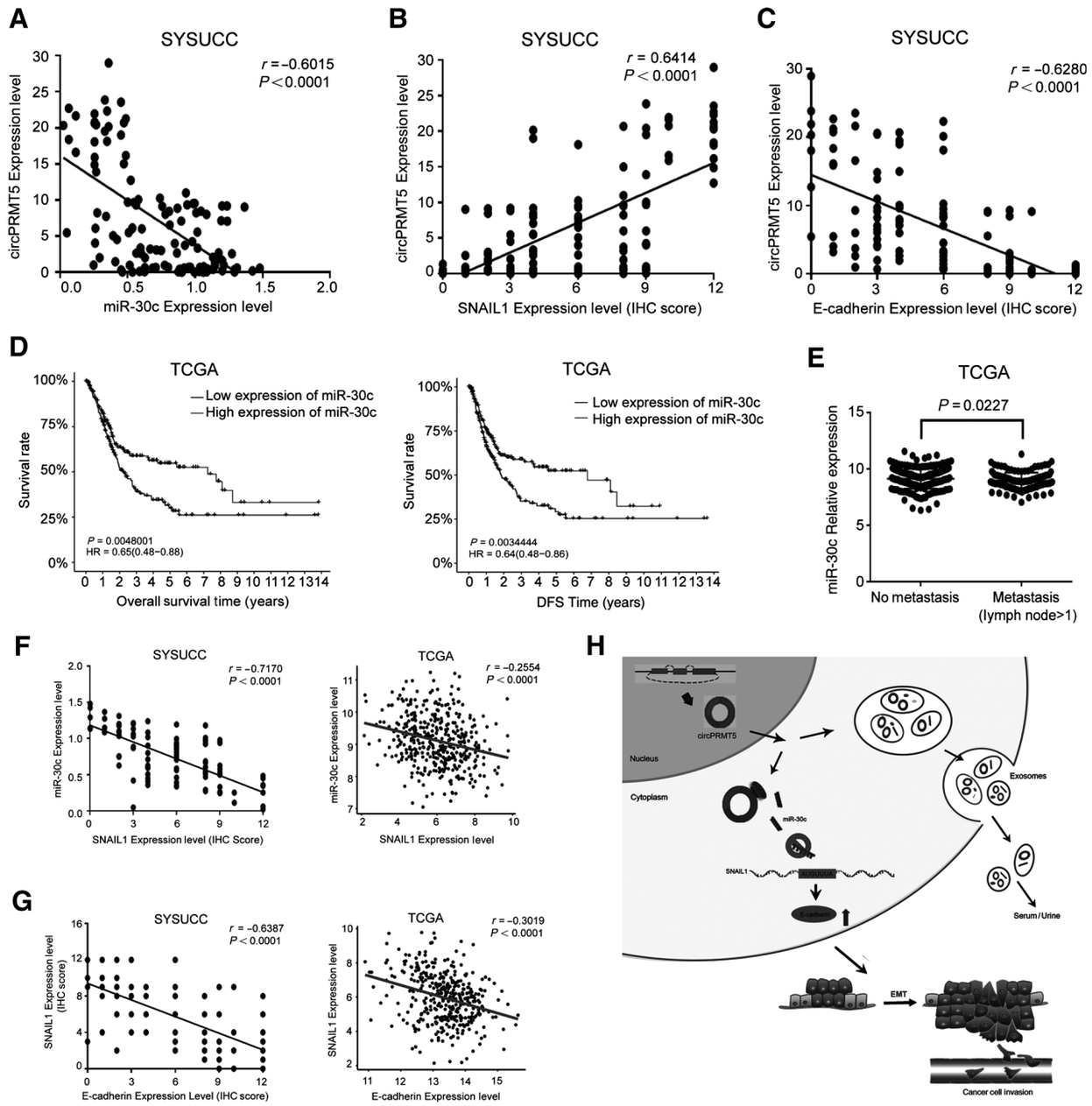

Figure 6.

CircPRMT5 regulated the miR-30c/SANIL1/E-cadherin pathway in patients with UCB. **A,** CircPRMT5 expression was negatively correlated with miR-30c expression in patients with UCB derived from SYSUCC. **B,** CircPRMT5 expression was positively correlated with SNAIL1 expression in patients with UCB derived from SYSUCC. **C,** CircPRMT5 expression was negatively correlated with E-cadherin expression in patients with UCB derived from SYSUCC. **D,** Kaplan–Meier curves with univariate analyses of overall survival (left) and DFS (right; **, $P < 0.01$, log-rank analysis) in patients with UCB with low versus high expression of miR-30c from TCGA cohorts. **E,** Scatter plots illustrating qRT-PCR analysis of expression fold change for miR30-c in UCB tissues with lymph node metastasis compared with those without metastasis from TCGA (right). *, $P < 0.05$, unpaired Student t test. **F,** miR-30c expression was negatively correlated with SNAIL1 expression in patients with UCB derived from SYSUCC (left) and TCGA (right). **G,** SNAIL1 expression was negatively correlated with E-cadherin in patients with UCB derived from SYSUCC (left) and TCGA (right). **H,** A proposed mechanistic model in which circPRMT5 functions as a miR-30c sponge and regulates SNAIL1/E-cadherin pathway via inhibiting miR-30c activity in UCB cells' EMT and invasion.

6F) and meanwhile, highly expressed SNAIL1 was significantly correlated with lower expressed E-cadherin (Fig. 6G; Supplementary Fig. S6). It has been identified that the expression of miR-200 family regulates EMT in UCB cells (25), and *SNAIL1* was shown as an important target of miR-200 family during EMT progression (26). We further analyzed the correlation between the expression of SNAIL1 and miR-200 family in the same UCB cohort derived from TCGA for comparison. As anticipated, a significantly inverse

correlation between the expression of SNAIL1 and miR-200 family (mir-200a and mir-200b) was evaluated in this UCB cohort ($r = -0.465$, $P < 0.001$; $r = -0.475$, $P < 0.001$, respectively, Supplementary Fig. S7). These data, taken together, suggest that miR-30c pathway in UCBs is essential for EMT progression of cancer cells.

CircPRMT5 is secreted by exosomes into serum and urine of patients with UCB and associated with tumor metastasis

Finally, in this study, we collected abundant serum samples from 71 patients with UCB and 36 normal people, and urine samples from 18 UCB patients and 14 normal people, respectively. After isolation of serum and urinary exosomes by sequential centrifugation, we characterized these vesicles by several methods such as electron microscopy (Supplementary Fig. S8A) and Western blot analysis (Supplementary Fig. S8B). The high presence of the exosomal markers CD63, TSG101, HSP70, and ALIX (27) confirmed the purity of isolated UCB-secreted exosomes in the serum and urine. qRT-PCR analyses showed that circPRMT5 was enriched in both serum and urinary exosomes derived from patients with UCB (Supplementary Fig. S8C and S8D, left), implying that highly expressed circPRMT5 in UCB might be secreted into tumor microenvironment, surrounding by blood vessels or urine. In addition, highly expressed circPRMT5 in the serum and urinary exosomes was positively correlated to lymph node metastasis and an advanced tumor progression (Supplementary Fig. S8C and S8D, right; Supplementary Table S4). Furthermore, there was a significant, inverse correlation between the expression levels of circPRMT5 and miR-30c in both serum and urinary exosomes derived from patients with UCB (Supplementary Fig. S8E and S8F).

Discussion

In this study, we first demonstrated that circPRMT5 was an important circRNA frequently upregulated in UCB tissue, and higher expression of circPRMT5 was positively correlated with UCB patients' metastasis and/or poorer survival. Second, from mechanistic study, we revealed that upregulation of circPRMT5 acted as the sponge of miR-30c and regulated the SNAIL1/E-cadherin pathway to promote UCB cells' EMT by competing for miR-30c. Third, we showed that overexpressed circPRMT5 was secreted by exosomes into the serum and urine of patients with UCB, predicting tumor lymph node metastasis. Given the importance of the SNAIL1/E-cadherin signaling in the progression of cancer cell's EMT (28), our results suggest, for the first time, the importance of circPRMT5 as a novel therapeutic target in human UCB.

Increasing evidence suggests that circRNAs are not simply the junk products in pre-mRNA splicing (29). A group of circRNAs have been reported to exert a regulatory role in diverse pathologic context. Dysregulated circRNAs have been reported in glioma (30), renal cell (31), lung (32), and other types of carcinomas (33). Our results clearly demonstrated that circPRMT5 was a frequently oncogenic event in UCB, contributing to the aggressive clinical UCB phenotype. Importantly, further functional studies showed that upregulated expression of circPRMT5 in UCB cells promoted cell's EMT and/or metastasis. Thus, in spite of tumor heterogeneity, the oncogenic role of circPRMT5 in EMT progression was strongly supported by our consistent clinical and both *in vitro* and *in vivo* studies.

Up to now, circRNAs have been well characterized to function as miRNA sponges (10). However, only a fraction of such circRNAs can trap a particular miRNA by multiple binding sites. Nevertheless, most of these studies lacked convictive experimental identification, and mainly focused on genome-wide bioinformatic analyses of all circRNA candidates. To better understand the regulatory mechanism of circPRMT5 in UCB cells' EMT and aggressive process, our data further showed that: (i) circPRMT5 was incorporated into AGO-RISC complex in UCB cells; (ii) circPRMT5 contained multiple miRNA-binding sites; (iii) circPRMT5 interacted with miR-30c in UCB cells. We agreed that numerous circRNAs with low abundance and small length may not work as miRNA sponges. Given the high expression of circPRMT5 in UCB, and based on these experimental evidences, we thus recommended that circPRMT5 might functionally act as the sponge for certain miRNAs, including miR-30c.

In the next parts of this study, we revealed that circPRMT5-induced UCB cells' EMT phenotype could be alleviated by enforced overexpression of miR-30c. The expression of circPRMT5 is negatively correlated with miR-30c expression in UCB tissues, supporting the critical regulatory role in metastasis by the circPRMT5-miR-30c regulatory axis. Furthermore, we showed that miR-30c was a critical negative regulator of the SNAIL1/E-cadherin–induced EMT pathway. Upregulated expression of circPRMT5 leaded to persistent activation of SNAIL1-induced EMT signaling in UCB cells and tissues, suggesting that circPRMT5 may enhance EMT-promoted UCB metastasis by blocking the miR-30c activity. So far, it has been reported that in lung cancer, miR-30c can also directly target certain oncogenes, Metadherin (*MTDH*) and the high-mobility group, AT-hook 2 (*HMGA2*) and the mesenchymal markers, vimentin (*VIM*) and fibronectin (*FN1*; ref. 34). In breast cancer, miR-30c acts as a tumor suppressor gene, targeting metastasis-associated protein 1 gene (*MTA1*; ref. 35). In this study, we further identified *SNAIL1* as a novel target regulated by miR-30c. These data, collectively, suggested a critical role of circPRMT5-sponged miR-30c in the control of cancer cell's EMT and/or invasiveness by means of a "one-hit/multiple-targets" mechanism.

It is noteworthy here, that in the last parts of our study, we found that the highly expressed circPRMT5 could be examined in serum and urine exosomes of patients with UCB. Although the presence of circRNAs in the serum exosome has been reported in patient with colorectal cancer and are powerful diagnostic biomarkers (15, 16), their pathologic roles require further determination. Herein, we found that circPRMT5 was significantly upregulated in both serum and urine exosomes derived from patients with UCB as compared with that from normal individual cohorts. Importantly, we identified that the serum and urine exosomes from patients with UCB contained higher expressed circPRMT5, which was not only positively associated with patients' lymph node metastasis, but also significantly correlated with the downregulated miR-30c. Taken together, these results reveal that the small "free" circRNAs, such as circPRMT5, which are highly stable *in vivo*, could be assembled into exosomes and exported to the extracellular microenvironment, including serum and urine, and predicts UCB patients' lymph node metastasis.

In summary, our report provides first line of comprehensive evidences that circPRMT5 is a novel oncogenic circRNA, as well as a prognostic biomarker in UCBs. CircPRMT5 exerts a bona fide regulatory role in blocking the activity of miR-30c, thereby involving in the SNAIL1-induced EMT pathway to support UCB cells' aggressive capacities, and it is illustrated in Fig. 6H. Clearly, our findings may offer a novel therapeutic target, circPRMT5, to broaden the treatment options for human UCB.

Disclosure of Potential Conflicts of Interest

No potential conflicts of interest were disclosed.

Authors' Contributions

Conception and design: X. Chen, F.-J. Zhou, D. Xie
Development of methodology: R. Chen, W.-S. Wei, Z.-H. Feng, L. Tan, S. Chen
Acquisition of data (provided animals, acquired and managed patients, provided facilities, etc.): Y.-H. Li, L. Tan, J.-W. Chen, G. Yuan, S. Chen, S.-J. Guo, K. Xiao, Z.-W. Liu, F.-J. Zhou
Analysis and interpretation of data (e.g., statistical analysis, biostatistics, computational analysis): W.-S. Wei, L. Tan, Z.-W. Liu, J.H. Luo, F.-J. Zhou
Writing, review, and/or revision of the manuscript: R. Chen, F.-J. Zhou, D. Xie
Administrative, technical, or material support (i.e., reporting or organizing data, constructing databases): X. Chen, R. Chen, F.-J. Zhou
Study supervision: F.-J. Zhou, D. Xie

Acknowledgments

We thank the TCGA research network for providing the data analyzed in this article. This study was supported by the grants from the National Key R&D Program of China (grant nos. 2017YFC1309001 and 2016YFC1302305, to D. Xie); the National Natural Science Foundation of China (grant No. 81602233, to X. Chen), 81672530 (to F.-J. Zhou), 81772726 (to Y.-H. Li), and 81730072 (to D. Xie); and the Natural Science Foundation of Guangdong Province (grant No. 2016A030310219; to X. Chen).

The costs of publication of this article were defrayed in part by the payment of page charges. This article must therefore be hereby marked *advertisement* in accordance with 18 U.S.C. Section 1734 solely to indicate this fact.

Received April 25, 2018; revised July 22, 2018; accepted August 23, 2018; published first October 10, 2018.

References

1. Jemal A, Bray F, Center MM, Ferlay J, Ward E, Forman D. Global cancer statistics. CA Cancer J Clin 2011;61:69–90.
2. Siegel R, Naishadham D, Jemal A. Cancer statistics, 2013. CA Cancer J Clin 2013;63:11–30.
3. Ashwal-Fluss R, Meyer M, Pamudurti NR, Ivanov A, Bartok O, Hanan M, et al. circRNA biogenesis competes with pre-mRNA splicing. Mol Cell 2014;56:55–66.
4. Starke S, Jost I, Rossbach O, Schneider T, Schreiner S, Hung LH, et al. Exon circularization requires canonical splice signals. Cell Rep 2015; 10:103–11.
5. Cocquerelle C, Mascrez B, Hetuin D, Bailleul B. Mis-splicing yields circular RNA molecules. FASEB J 1993;7:155–60.
6. Capel B, Swain A, Nicolis S, Hacker A, Walter M, Koopman P, et al. Circular transcripts of the testis-determining gene Sry in adult mouse testis. Cell 1993;73:1019–30.
7. Memczak S, Jens M, Elefsinioti A, Torti F, Krueger J, Rybak A, et al. Circular RNAs are a large class of animal RNAs with regulatory potency. Nature 2013;495:333–8.
8. Lu T, Cui L, Zhou Y, Zhu C, Fan D, Gong H, et al. Transcriptome-wide investigation of circular RNAs in rice. RNA 2015;21:2076–87.
9. Jeck WR, Sorrentino JA, Wang K, Slevin MK, Burd CE, Liu J, et al. Circular RNAs are abundant, conserved, and associated with ALU repeats. RNA 2013;19:141–57.
10. Hansen TB, Jensen TI, Clausen BH, Bramsen JB, Finsen B, Damgaard CK, et al. Natural RNA circles function as efficient microRNA sponges. Nature 2013;495:384–8.
11. Zheng Q, Bao C, Guo W, Li S, Chen J, Chen B, et al. Circular RNA profiling reveals an abundant circHIPK3 that regulates cell growth by sponging multiple miRNAs. Nat Commun 2016;7:11215.
12. Yu J, Xu QG, Wang ZG, Yang Y, Zhang L, Ma JZ, et al. Circular RNA cSMARCA5 inhibits growth and metastasis in hepatocellular carcinoma. J Hepatol 2018;68:1214–27.
13. Pan BT, Teng K, Wu C, Adam M, Johnstone RM. Electron microscopic evidence for externalization of the transferrin receptor in vesicular form in sheep reticulocytes. J Cell Biol 1985;101:942–8.
14. Becker A, Thakur BK, Weiss JM, Kim HS, Peinado H, Lyden D. Extracellular vesicles in cancer: cell-to-cell mediators of metastasis. Cancer Cell 2016;30:836–48.
15. Li Y, Zheng Q, Bao C, Li S, Guo W, Zhao J, et al. Circular RNA is enriched and stable in exosomes: a promising biomarker for cancer diagnosis. Cell Res 2015;25:981–4.
16. Dou Y, Cha DJ, Franklin JL, Higginbotham JN, Jeppesen DK, Weaver AM, et al. Circular RNAs are down-regulated in KRAS mutant colon cancer cells and can be transferred to exosomes. Sci Rep 2016;6: 37982.
17. Street JM, Yuen PS, Star RA. Bioactive exosomes: possibilities for diagnosis and management of bladder cancer. J Urol 2014;192:297–8.
18. Nawaz M, Camussi G, Valadi H, Nazarenko I, Ekstrom K, Wang X, et al. The emerging role of extracellular vesicles as biomarkers for urogenital cancers. Nat Rev Urol 2014;11:688–701.
19. Wittekind C. [2010 TNM system: on the 7th edition of TNM classification of malignant tumors]. Pathologe 2010;31:331–2.
20. Yu C, Liu Z, Chen Q, Li Y, Jiang L, Zhang Z, et al. Nkx2.8 inhibits epithelial-mesenchymal transition in bladder urothelial carcinoma via transcriptional repression of twist1. Cancer Res 2018;78:1241–52.
21. Li Z, Huang C, Bao C, Chen L, Lin M, Wang X, et al. Exon-intron circular RNAs regulate transcription in the nucleus. Nat Struct Mol Biol 2015;22:256–64.
22. Agarwal V, Bell GW, Nam JW, Bartel DP. Predicting effective microRNA target sites in mammalian mRNAs. eLife 2015;4:e05005.
23. Betel D, Koppal A, Agius P, Sander C, Leslie C. Comprehensive modeling of microRNA targets predicts functional non-conserved and non-canonical sites. Genome Biol 2010;11:R90.
24. Herranz N, Pasini D, Diaz VM, Franci C, Gutierrez A, Dave N, et al. Polycomb complex 2 is required for E-cadherin repression by the Snail1 transcription factor. Mol Cell Biol 2008;28:4772–81.
25. Adam L, Zhong M, Choi W, Qi W, Nicoloso M, Arora A, et al. miR-200 expression regulates epithelial-to-mesenchymal transition in bladder cancer cells and reverses resistance to epidermal growth factor receptor therapy. Clin Cancer Res 2009;15:5060–72.
26. Perdigao-Henriques R, Petrocca F, Altschuler G, Thomas MP, Le MT, Tan SM, et al. miR-200 promotes the mesenchymal to epithelial transition by suppressing multiple members of the Zeb2 and Snail1 transcriptional repressor complexes. Oncogene 2016;35:158–72.
27. Taylor DD, Gercel-Taylor C. Exosomes/microvesicles: mediators of cancer-associated immunosuppressive microenvironments. Semin Immunopathol 2011;33:441–54.
28. Kaufhold S, Bonavida B. Central role of Snail1 in the regulation of EMT and resistance in cancer: a target for therapeutic intervention. J Exp Clin Cancer Res 2014;33:62.
29. Chen LL. The biogenesis and emerging roles of circular RNAs. Nat Rev Mol Cell Biol 2016;17:205–11.
30. Yang Y, Gao X, Zhang M, Yan S, Sun C, Xiao F, et al. Novel role of FBXW7 circular RNA in repressing glioma tumorigenesis. J Natl Cancer Inst 2018;110:Jul 6. doi: 10.1093/jnci/djy118. [Epub ahead of print].
31. Wang K, Sun Y, Tao W, Fei X, Chang C. Androgen receptor (AR) promotes clear cell renal cell carcinoma (ccRCC) migration and invasion via altering the circHIAT1/miR-195-5p/29a-3p/29c-3p/CDC42 signals. Cancer Lett 2017;394:1–12.
32. Qiu M, Xia W, Chen R, Wang S, Xu Y, Ma Z, et al. The circular RNA circPRKCI promotes tumor growth in lung adenocarcinoma. Cancer Res 2018; 78:2839–51.
33. Hansen TB, Kjems J, Damgaard CK. Circular RNA and miR-7 in cancer. Cancer Res 2013;73:5609–12.
34. Suh SS, Yoo JY, Cui R, Kaur B, Huebner K, Lee TK, et al. FHIT suppresses epithelial-mesenchymal transition (EMT) and metastasis in lung cancer through modulation of microRNAs. PLos Genet 2014;10:e1004652.
35. Wang X, Qiu LW, Peng C, Zhong SP, Ye L, Wang D. MicroRNA-30c inhibits metastasis of ovarian cancer by targeting metastasis-associated gene 1. J Cancer Res Ther 2017;13:676–82.